Porter, R. (2017). Cloaking in Water Waves. In *World Scientific Handbook of Metamaterials and Plasmonics* (World Scientific Handbook of Metamaterials and Plasmonics cover World Scientific Series in Nanoscience and Nanotechnology; Vol. 2). World Scientific Publishing Co.. https://doi.org/10.1142/9789813228702_0009

Peer reviewed version

Cloaking in water waves

R. Porter

School of Mathematics, University Walk, University of Bristol, BS8 1TW, UK.

1 Introduction

This review article is written with two goals in mind. The first is to provide researchers working in the area of water waves an insight into ideas emerging from the physics community on the use of metamaterials in controlling waves in unusual ways. The second is to give physicists already familiar with these ideas an overview of the theory of water waves, the common approximations that are used in developing solutions, and how metamaterial concepts may be implemented within this framework.

In particular, whilst there has been an expansive crossover of ideas developed primarily from optics and electromagnetics into the acoustics and elasticity research communities, much less has been realised in terms of establishing such a connection in the water wave community.

There is a good reason why this might be. Water waves are quite different to waves in electromagnetics, acoustics or elasticity in that there is a special direction (the vertical) which makes simple connections between theories less easy to establish: the limitations imposed by a free surface and a fluid depth are a recurring theme throughout this article. The applications of metamaterials in water waves are also perhaps a little harder to imagine. On the other hand wave phenomena are easily visualised on the surface of water and this makes it an attractive medium in which to develop ideas from other areas of physics.

My own interest in this subject was stimulated after becoming aware of the publication of the work of [11] Immediately evident was the widespread influence of the work of [30] and [19] on invisibility cloaking in optics and other extensions to areas of science including acoustics and elasticity. Although I've not fully engaged with metamaterial science I've slowly picked up many of the intruiging developments that have been made over the last 15–20

years, especially those with applications in water waves. Broadly speaking, a metamaterial is a medium in which properties of a field can be propagated in a manner not normally found in natural materials. They are most often comprised of microstructures much smaller than the natural lengthscales intrinsic to the underlying field variables in such a way that their macroscopic effect on the field allows complex phenomena to be exhibited. These include negative refraction in which oblique waves bend backwards as they enter the metamaterial and perfect lensing, e.g. [28] and [36]. In the context of water waves, see [13].

One of the most fascinating areas to emerge from the science of metamaterials is invisibility cloaking in which obstacles are rendered undetectable to the observer and it is principally on this topic which the current article will focus. It turns out that the capacity to cloak in water waves leads to a reduction (to zero for a perfect cloak) of the so-called mean drift force. This is a second-order effect in water waves and hence generally smaller in magnitude than the primary oscillatory forces due to water waves but, unlike those wave forces, it is steady and has important consequences in the design of marine structures such as the foundations of offshore wind turbines.

The layout of the article is as follows. In the remainder of this section, we shall introduce the underlying equations of motion which govern small-amplitude water waves and apply it to our canonical problem of the scattering by a vertical cylinder. In §2, a series of approximations to the full governing equation in which the depth dependence is removed will be introduced and discussed in the context of cloaking cylinders. §3 describes the transformation media approach and how it applies to depth-averaged models. This includes a discussion of how to design the metamaterials needed to practically implement the wave control needed to cloak. In §4 we consider examples of cloaking in the unapproximated full linear theory and the work is summarised in §5.

1.1 Linearised theory of water waves

There are many textbooks which carefully outline the derivation of the linearised theory of water waves which we summarise below. It is hard to beat the account in the book of [24] and we refer to this extensively throughout.

Throughout this article we take z to be the vertical axis with $z = 0$ set to the level of the undisturbed free surface. A fluid of density ρ under the influence of gravity g lies below $z = 0$ in equilibrium and is bounded below

by an impermeable bed at $z = -h(x, y)$ where (x, y) are the horizontal coordinates. It is assumed in deriving conditions at the free surface that a fluid (such as the air) having density much less than ρ and in which the pressure is constant lies above $z = 0$ in equilibrium. The effect of this fluid on the motion of the water is then negligible.

There are many other assumptions used in the derivation of classical water wave theory. The first is that the fluid is inviscid. This is a good assumption in the bulk but fails close to boundaries, including on the free surface – see [24, §9]. However, it is a good approximation overall provided any experimental realisation of the theory is performed on a large enough scale. Another assumption is that the flow is irrotational (implying there is no vorticity in the fluid). In order that theory can be realised in experiments this often implies avoiding geometrical structures with sharp corners or edges which induce vortex shedding. Irrotationality implies velocity of the fluid $\mathbf{u}(x, y, z, t)$ satisfies the condition $\nabla \times \mathbf{u} = 0$ which allows us to write $\mathbf{u} = \nabla\Phi(x, y, z, t)$ where Φ is a scalar potential (called the velocity potential) and $\nabla = (\partial_x, \partial_y, \partial_z)$. Further, it is routine to assume that the water is incompressible and this is expressed mathematically as $\nabla \cdot \mathbf{u} = 0$. Consequently, Φ satisfies

$$\nabla^2\Phi = 0, \qquad \text{in } \mathcal{V} \tag{1}$$

where $\mathcal{V}$ represents the domain occupied by the fluid and $\nabla^2 = \nabla \cdot \nabla$ is the three-dimensional Laplacian.

Euler's equation expressing conservation of momentum for an inviscid fluid allows the pressure to be determined in the fluid. Setting this constant on the free surface and linearising on the assumption of small steepness of the surface elevation defined by $z = \zeta(x, y, t)$ about the mean level furnishes the dynamic boundary condition

$$\Phi_t + g\zeta = 0, \qquad \text{on } z = 0. \tag{2}$$

Similarly, a linearised version of the kinematic condition on the surface, which states that the surface moves with the fluid, gives

$$\zeta_t = \Phi_z, \qquad \text{on } z = 0. \tag{3}$$

The two equations (2) and (3) can be combined to eliminate ζ so that

$$\Phi_{tt} + g\Phi = 0, \qquad \text{on } z = 0 \tag{4}$$

expresses a combined kinematic and dynamic boundary condition. The condition that there is no flow through all fixed wetted boundaries $\mathcal{S}$ with given unit normal $\mathbf{n}$ out of the fluid implies that

$$\Phi_n \equiv \mathbf{n} \cdot \nabla \Phi = 0, \qquad \text{on } (x, y, z) \in \mathcal{S}. \tag{5}$$

One section of $\mathcal{S}$ is the sea bed where $\mathbf{n} = (h_x, h_y, -1)$ and (5) reduces to

$$\Phi_z + \nabla_h h \cdot \nabla_h \Phi = 0, \qquad \text{on } z = -h(x, y) \tag{6}$$

where $\nabla_h \equiv (\partial_x, \partial_y)$ is the gradient projected onto the two-dimensional horizontal plane. The bed is often assumed to be flat outside some bounded region of the (x, y)-plane, and given by $h = h_0$, a constant, and there (6) reduces to

$$\Phi_z = 0, \qquad \text{on } z = -h_0. \tag{7}$$

In order to fully specify a problem which can be solved (numerically or analytically) one must also impose initial conditions. These most often imply stating the initial surface elevation and velocity at a reference time $t = 0$. However advantage can be (and most often is) taken of the fact that the governing equation for Φ and the boundary condition it satisfies are linear and so any time domain solution can be inferred via inverse Fourier transforms of frequency domain solutions. Thus, we write $\Phi(x, y, z, t) = \Re\{\phi(x, y, z)\mathrm{e}^{-\mathrm{i}\omega t}\}$ and $\zeta(x, y, t) = \Re\{\eta(x, y)\mathrm{e}^{-\mathrm{i}\omega t}\}$ where ω is the assumed radian frequency and now ϕ and η are frequency-dependent complex-valued functions incorporating information about the amplitude and the phase of the fluid motion.

It follows from (1), (4) and (5) that ϕ now satisfies

$$\nabla^2 \phi = 0, \qquad \text{in } \mathcal{V} \tag{8}$$

with

$$\phi_z - K\phi = 0, \qquad \text{on } z = 0 \tag{9}$$

where $K = \omega^2/g$ and

$$\phi_n = 0, \qquad \text{on } \mathcal{S} \tag{10}$$

which includes (6) in the form

$$\phi_z + \nabla_h h \cdot \nabla_h \phi = 0, \qquad \text{on } z = -h(x, y) \tag{11}$$

simplifying (7) to $\phi_z = 0$ on $z = -h_0$ where the bed is flat. Also (2) translates to

$$\eta(x, y) = (\mathrm{i}\omega/g)\phi(x, y, 0) \tag{12}$$

representing the time-independent free-surface elevation.

1.2 The character of waves

Waves propagate on the surface of the water (they are akin to guided, interface or surface waves in other physical disciplines) with exponential decay in the direction of increasing depth away from the surface. Waves of amplitude A over a flat bed of depth h_0 from infinity in a direction θ_0 w.r.t. the positive x-axis are given by the potential

$$\phi_{inc} = \frac{-\mathrm{i}gA}{\omega}\frac{\cosh k_0(z+h_0)}{\cosh k_0 h_0}\mathrm{e}^{\mathrm{i}k_0(x\cos\theta_0+y\sin\theta_0)}. \tag{13}$$

This satisfies (8) and (11) on $z = -h_0$ and (9) provided that the unique positive real root k of

$$K \equiv \frac{\omega^2}{g} = k\tanh kh \tag{14}$$

corresponding to $h = h_0$ is assigned to k_0. The equation (14) is called the water wave dispersion relation and encodes information on how waves of different frequencies travel at different speeds and how both relate to the fluid depth. As usual, the phase speed is given by $c = \omega/k$ and the group velocity has magnitude $c_g = \mathrm{d}\omega/\mathrm{d}k$.

We shall refer to the shallow water regime as being when $kh \ll 1$ or $\lambda \gg h$ where $\lambda = 2\pi/k$ is the wavelength. In this case (14) shows that $k \approx \omega/\sqrt{gh}$ and $c \approx \sqrt{gh}$ whilst $c_g \approx c$. Water waves are therefore non-dispersive in the shallow water approximation. On the other hand in the deep water regime, $kh \gg 1$ or $\lambda \ll h$, (14) shows that $k \approx \omega^2/g$ and $c \approx g/\omega$ with $c_g \approx \frac{1}{2}c$.

In many applications of linear wave theory one is interested in how an incident plane wave as described by (13) interacts with fixed or moving marine structures such as the legs of an oil rig, an offshore breakwater, varying bathymetry, the coast, ships or wave energy absorbing devices.

1.3 Scattering by a vertical circular cylinder

Even with the simplifying assumptions that comprise the linearised theory of water waves, the three-dimensional boundary-value problem is complicated and substantial analytic progress is often restricted to a small class of problems with a simple geometric configuration. Many of these are posed in a two-dimensional reduction of the water wave problem in which plane parallel-crested waves are incident on a geometry which has constant cross-section in one horizontal direction. In such problems wave propagation is essentially

one-dimensional and confined to the other perpendicular horizontal direction. Thus, wave scattering problems are reduced to determining a reflection and a transmission coefficient.

Undoubtably the simplest non-trivial problem to consider analytically in three dimensions involves the scattering by a circular cylinder of constant cross section protruding vertically from a bed of constant depth h_0 through the surface of the fluid. This problem forms the basis of much of what is to come in the rest of this article and it is instructive to use it as an example of the theory introduced so far.

It is natural to use cylindrical coordinates $x = r\cos\theta$, $y = r\sin\theta$. Then it can be shown that

$$\phi_{inc} = \mathrm{e}^{\mathrm{i}k_0 r\cos(\theta-\theta_0)}\cosh k_0(z+h_0) = \cosh k_0(z+h_0)\sum_{n=-\infty}^{\infty}\mathrm{i}^n J_n(k_0 r)\mathrm{e}^{\mathrm{i}n(\theta-\theta_0)}. \tag{15}$$

where J_n are Bessel functions. Note that here and henceforth we dismiss the constant prefactor in (13) for clarity as the problem is linear and solutions can be scaled *a posteriori* as necessary.

The fact that cylinder surface (radius a, say) is aligned with the vertical and extends throughout the depth means that the scattered wave response to the incident wave has the same depth dependence as the incident wave (we elaborate on this in a moment). The total diffracted field is $\phi = \phi_{inc} + \phi_s$ where

$$\phi_s = \cosh k_0(z+h_0)\sum_{n=-\infty}^{\infty} a_n H_n^{(1)}(k_0 r)\mathrm{e}^{\mathrm{i}n(\theta-\theta_0)} \tag{16}$$

and a_n are as yet unknown Fourier-Bessel coefficients. The potential in (16), derived by separation of variables, satisfies (8), (9) and (11) where $H_n^{(1)}(z) = J_n(z) + \mathrm{i}Y_n(z)$ is the Hankel function of the first kind. This choice, rather than any other combination of Bessel functions, ensures that the scattered potential represents outgoing waves at infinity. This so-called radiation condition is a previously unstated requirement in the specification of the water wave boundary-value problem posed in the frequency domain.

Upon satisfaction of the cylinder boundary condition (10), which here is $\phi_r = 0$ on $r = a$, for all $-h_0 < z < 0$, $-\pi < \theta \leq \pi$ determines

$$a_n = -\mathrm{i}^n \frac{J_n'(k_0 a)}{H_n^{(1)\prime}(k_0 a)} \tag{17}$$

and the solution is complete. The solution $\phi = \phi_{inc} + \phi_s$ formed from (15), (16) and (17) is attributed to [22] amongst researchers in the water waves although it is familiar in other areas of physics.

As already indicated the geometry in this problem, which is comprised of a flat bed and vertically-walled scatterers, means that $\cosh k_0(z+h_0)$ can be factorised from the potential as

$$\phi(x,y,z) = \psi(x,y)\cosh k_0(z+h_0) \tag{18}$$

and (8) reduces to the two-dimensional wave equation

$$(\nabla_h^2 + k_0^2)\psi = 0 \tag{19}$$

which shares solutions common to scalar TE- and TM-polarised waves in electromagnetics and two-dimensional inviscid low-Mach number acoustics. Unlike those physical disciplines, in water waves where Neumann boundary conditions represent fixed impermable boundaries, there is no physical realisation of a boundary which has a Dirichlet condition imposed upon it. Boundary conditions of the form $\phi_n + \alpha\phi = 0$, $\alpha \in \mathbb{C}$ are used in fluids to represent dissipative surfaces such as rough walls or porous membranes.

As a brief aside, if the cylinder were truncated and did not extend throughout the entire fluid depth, the reduction made in (19) would not be possible. Instead, one would have to expand the scattering potential outside the cylinder $r > a$ in a complete set of depth modes (see [25], for example) which are defined by the infinite sequence of imaginary roots of (14). The additional depth modes in the series correspond to spatially evanescent or localised waves which decay exponentially away from the scatterer. As shown in [25] this solution would have to be matched to a series representation of the potential in the fluid region in $r < a$ no longer occupied by the vertical cylinder.

Although we shall make some small diversions along the way, the main thrust of this article will concern how to cloak a circular cylinder extending through the depth. By cloak, we shall mean that an observer suitably far away from the cylinder cannot detect the presence of the cylinder by monitoring the wave field. In other words, we require that there is no energy scattered in any direction away from the cylinder.

Returning to (16), (17) and letting $k_0 r \to \infty$ we have

$$\phi_s \sim \sqrt{\frac{2}{\pi k_0 r}}\mathrm{e}^{\mathrm{i}k_0 r - \mathrm{i}\pi/4}\mathcal{A}(\theta;\theta_0)\cosh k_0(z+h_0) \tag{20}$$

representing an outgoing circular wave field with amplitude in the θ direction due to an incident wave propagating in the direction θ_0 given by

$$\mathcal{A}(\theta;\theta_0) = -\sum_{n=-\infty}^{\infty} \frac{J_n'(k_0 a)}{H_n^{(1)'}(k_0 a)} \mathrm{e}^{\mathrm{i}n(\theta-\theta_0)}. \tag{21}$$

after using the large argument asymptotics of the Hankel function. The total scattered energy – or scattering cross-section – is defined here as

$$\sigma = \frac{1}{2\pi}\int_{-\pi}^{\pi} |\mathcal{A}(\theta;\theta_0)|^2 \,\mathrm{d}\theta = -\Re\{\mathcal{A}(\theta_0;\theta_0)\}. \tag{22}$$

The final equality, originally derived by [21] in the water wave context, is familiar in physics and known as the optical theorem. Either of the two definitions of σ in (22) can by used with (20) to show that

$$\sigma_{cyl} = \sum_{n=-\infty}^{\infty} \left| \frac{J_n'(k_0 a)}{H_n^{(1)'}(k_0 a)} \right|^2 \tag{23}$$

and this is never zero for any $k_0 a$, i.e. a cylinder will always scatter energy (e.g. see Fig. 3(a)).

We now consider a range of possibilities for cloaking a cylinder. Following the pioneering papers of [30] and [19] the principle idea in cloaking is to alter the material parameters of a property within a domain exterior to the object being cloaked in such a way to bend waves around that object. There are a number of possibilities that will be considered in this regard. A natural starting point is to exploit the fact that waves refract under a change in depth; one can observe oblique waves straighten up as the approach the shoreline of a shallow beach.

Much of the complication we encounter lies in the fact that the water wave problem is inherently three-dimensional with one special direction (the vertical) and has boundaries defined by the free surface and the sea bed.

Thus, initially we shall consider a number of reduced models – approximations to the governing equations – which remove this complication.

2 Two-dimensional approximations to the full theory

2.1 Ray theory

We can consider an approximation to the three-dimensional water wave scattering problem based on ray theory (or geometric optics). In this approach, the effects of refraction due to changes in the depth are captured but diffraction is not. The basis of the approximation is that the wavelength is assumed to be much smaller than the length scale of horizontal bottom variations. In other words, $|\nabla_h h|/kh \ll 1$. Then (following [24, §3.1,§3.2] for example), a multiple scales approach can be used to derive the Eikonal equation familiar in optics and acoustics:

$$S_x^2 + S_y^2 = k^2 \tag{24}$$

where k is the wavenumber satisfying (14). Here, $S(x, y) = constant$ represent lines of constant phase and wave rays follow paths that are perpendicular to these lines. Normally one might prescribe a depth variation $h(x, y)$ which, through (14) would define a wavenumber variation $k = k(h)$ and then solve (24) for S and hence determine the ray paths – see [24, §3.3,§3.4] for examples of how this done.

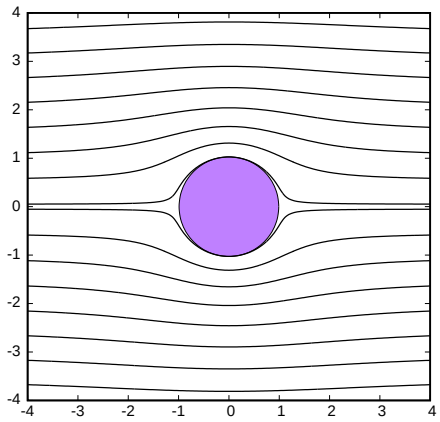

Figure 1: Ray paths according to (26) around the cylinder radius $a = 1$.

However we can also consider an inverse approach whereby the function $S(x, y)$ is prescribed and we infer a depth variation from (14). To cloak a

cylinder of radius a, rays will need to be bent around the cylinder by changes in depth and so we will require $S \to k_0 x$ at large distances and $S_r = 0$ on $r = a$. That is, the rays are to be parallel and aligned with the x direction at large distances where the depth is assumed to tend to h_0 whilst lines of constant phase are perpendicular to the cylinder on its surface. The simplest (but not the only) choice of function satisfying these requirements is, in polar coordinates,

$$S(r, \theta) = k_0 r \cos\theta + k_0 a^2 \cos\theta / r \tag{25}$$

which is equivalent to the potential for the streaming flow of an inviscid irrotational fluid past a circle. Since S is a harmonic function the conjugate function provides us with the ray paths. Thus these are given by

$$k_0 r \sin\theta - k_0 a^2 \sin\theta / r = constant. \tag{26}$$

It follows from using (25) in (24) that

$$k^2 = k_0^2 \left(1 + \frac{a^4}{r^4} - \frac{2a^2}{r^2}\cos 2\theta\right) \equiv k_0^2 F^2. \tag{27}$$

Although there is no restriction on the range of values of kh in this theory, if we make the assumption $kh \ll 1$ everywhere in the domain then we can use the shallow water dispersion relation to give

$$\frac{h}{h_0} = \frac{1}{F^2}. \tag{28}$$

This formula predicts infinite depth at the 'singular points' $(\pm a, 0)$ fore and aft of the cylinder. On physical reasoning this is to be expected and these are also points singularities in other solutions to cloaking problems including those proposed by [30]. The main difficulty here is that $|\nabla_h h| \not\ll kh$ nor $kh \not\ll 1$ in large areas fore and aft of the cylinder and the basis of the approximation is violated. See Fig. 2(a) where the red coloured lobes represent depths greater than six times the depth in the far-field.

Using the full dispersion relation (14) instead of the shallow water version allows us to extend the range of values kh can take and then

$$h = \frac{1}{k_0 F} \tanh^{-1}\left(\frac{\tanh k_0 h_0}{F}\right). \tag{29}$$

Now h is undefined for values of (r, θ) such that $F < \tanh k_0 h_0$. These emerge fore and aft of the cylinder – in Fig. 2(b) they are represented by the two white lobes.

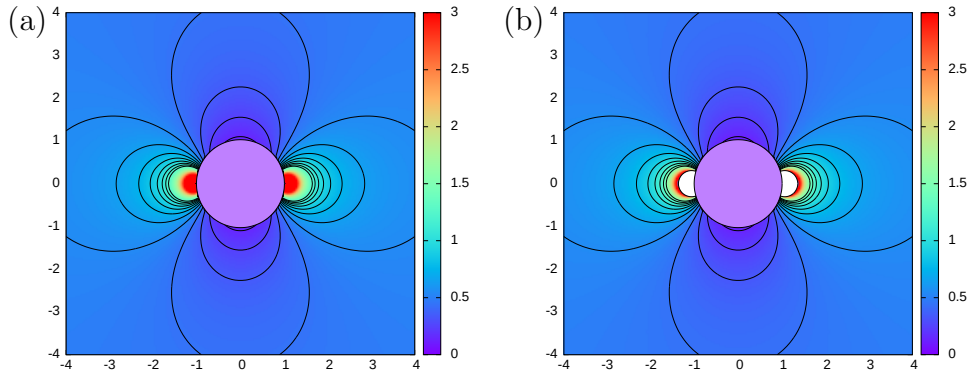

Figure 2: The depth profiles around the cylinder radius $a = 1$, $h_0 = \frac{1}{2}$ under ray theory assuming: (a) shallow water defined by (28); (b) unrestricted depth defined by (29) with $k_0 = 1$.

Other more exotic versions of the phase function can be used (S is certainly not required to be harmonic) provided they satisfy the two requirements stated earlier. Numerical experiments suggest that issues of large gradients and regions of undefined depth that invalidate these solutions cannot be overcome.

2.2 Shallow water equations

There are two common ways of deriving the linearised shallow water equations (or linearised long wave equations). One is to return to principles of fluid dynamics and make a shallow depth approximation from the outset. We shall adopt this approach later. The other is to apply the approximation directly to the full three-dimensional governing equations presented in §1.1. For a formal derivation based on this latter approach one can follow [24, §4.1] who rescales coordinates on physical lengthscales and then performs an asymptotic expansion of the potential in a small parameter $|\nabla_h h|/kh$. This is all performed under the assumption $kh \ll 1$ so that (14) is replaced locally by $k^2 \approx \omega^2/(gh)$. and gives rise to the linear Shallow Water Equation

$$\nabla_h \cdot (h \nabla_h \eta) + \frac{\omega^2}{g} \eta = 0 \tag{30}$$

for the surface wave elevation, $\eta(x, y)$ defined by (12). If the depth is constant and $h = h_0$ then (30) reduces to the two-dimensional wave equation

$$\nabla_h^2 \eta + k_0^2 \eta = 0 \tag{31}$$

which we have seen in (18) can be applied at any depth, not just when $k_0 h_0 \ll 1$ and waves propagating in the positive x direction are given by $\eta = \mathrm{e}^{\mathrm{i}k_0 x}$.

By writing $\eta = h^{-1/2}\overline{\eta}$ we can transform (30) into its canonical form

$$\nabla_h^2 \overline{\eta} + k_0^2 n^2 \overline{\eta} = 0 \tag{32}$$

where

$$n^2 = \frac{h_0}{h}\left(1 + \frac{|\nabla_h h|^2}{4k^2h^2} - \frac{\nabla_h^2 h}{2k^2 h}\right) \tag{33}$$

acts as a refractive index dependent upon the depth.

2.3 Conformal mapping

Following [19] we can introduce a conformal mapping from the physical (x, y) plane into a new (u, v) plane via $\beta = f(\xi)$ where $\beta = u + \mathrm{i}v$ and $\xi = x + \mathrm{i}y$. Under the transformation,

$$\nabla_h^2 \equiv \partial_\xi \partial_{\xi^*} = |f'(\xi)|^2 \partial_\beta \partial_{\beta^*} \equiv |f'(\xi)|^2 \widetilde{\nabla}_h^2 \tag{34}$$

where $\widetilde{\nabla}_h^2 = \partial_{uu} + \partial_{vv}$ Thus (34) is mapped to

$$\widetilde{\nabla}_h^2 \widetilde{\eta} + k_0^2 \widetilde{n}^2 \widetilde{\eta} = 0 \tag{35}$$

where $\widetilde{\eta}(u, v) \equiv \overline{\eta}(x, y)$ and

$$\widetilde{n}^2(u, v) = n^2(x, y)/|f'(\xi)|^2 \tag{36}$$

and so the transformation preserves the structure of the shallow water equation whilst the refractive index is transformed by the mapping.

In terms of cloaking a cylinder, we can introduce a conformal transformation

$$f(\xi) = \xi + a^2/\xi \tag{37}$$

which maps the cylinder $|\xi| = a$ onto the line $-2a < u < 2a$, $v = 0$ in the β-plane. Thus, if $h = h_0$ in the mapped system so that $\widetilde{n} = 1$ with the solution

$\widetilde{\eta}(u,v) = \mathrm{e}^{\mathrm{i}k_0 u}$ representing waves propagating without distortion past the line $-2a < u < 2a$, $v = 0$, then the mapping (37) gives us the Shallow Water Equation (35) for waves deflected past a cylinder of radius a with a depth profile h defined by

$$|1 - a^2/\xi^2|^2 = \frac{h_0}{h}\left(1 + \frac{|\nabla_h h|^2}{4k^2h^2} - \frac{\nabla_h^2 h}{2k^2 h}\right). \tag{38}$$

This nonlinear PDE would have to be solved for h outside $r = a$. It is not clear (at least to the author) how this would be done, and it may not be possible to define a function h which satisfies (38) everywhere.

We note in passing that if one chooses to return to (33) and make it more tractable by neglecting derivatives of h (justified, perhaps, because it shallow water approximation demands small gradients) then the right-hand side term in (38) becomes h_0/h and so with $\xi = r\mathrm{e}^{\mathrm{i}\theta}$, (38) is the same as (28) which we arrived at by taking a shallow water approximation to ray theory. This is an unsurprising outcome.

As was observed in §2.1 the difficulty here is that the map (37) which transforms a line in Cartesian coordinates to the exterior of the circle creates variations in the depth which violate the assumptions of the model.

We remark however that this method can be useful in other applications where one wishes to control waves. Recently, for example, [40] have used this method to bend, focus and directionally radiate waves. Also recently, [5] has used conformal mappings of parallel waveguides into meandering waveguides. Here the distortion to the bed created by the mapping is small and the argument that higher order terms in (38) can be approximately neglected is valid. Thus $h = h_0/|f'(\xi)|^2$ is exactly the mapping of [5] to show that waves can be perfectly transmitted with no reflection along a meandering waveguide.

We return to the Shallow Water Equations later.

2.4 The Mild-Slope Equations

This is a good point at which to briefly mention an alternative reduced model which is more sophisticated than the shallow water approximation but retains its structure. Crucially, it is valid for all kh although still restricted by $|\nabla_h h|/kh \ll 1$. Thus the limitation $kh \ll 1$ of shallow water theory is removed. As in shallow water theory, the basis of the approximation is that

bed gradients are small enough to suppose the bed is locally flat. Thus, whilst h varies globally, locally we assume the separable representation, inspired by the fact that (18) is exact for a flat bed,

$$\phi(x, y, z) \approx \psi(x, y) \cosh k(z + h) \tag{39}$$

where $k = k(h(x, y))$ is now determined locally by the dispersion relation (14). There are many derivations, variants and extensions of the Mild-Slope Equations (MSEs), originally attributed to [3] and [37]. This partly reflects the rather ad hoc nature of the approximation. See [24, §3.5] for a derivation which shows the depth averaging process in action. For a more formal approach which is underpinned by a variational principle, see [7]. That work resulted in the so-called Modified Mild-Slope Equations (MMSE) which retained terms proportional to the gradient and curvature of the bed neglected in previous derivations. Thus, the MMSE is given by

$$\nabla_h \cdot (u_0 \nabla_h \psi) + (k^2 + u_1 |\nabla_h h|^2 + u_2 \nabla_h^2 h)\psi = 0 \tag{40}$$

where $u_0 = cc_g$ (the product of phase speed and group velocity), u_1 and u_2 are defined in [7]. and restated in [24, §3.5] in terms of the local depth h; the surface elevation η is a scaled function of ψ. As in §2.2 a transformation into canonical form can be achieved by writing $\psi = u_0^{-1/2}\overline{\psi}$ so that (40) becomes

$$\nabla_h^2 \overline{\psi} + k_0^2 n^2 \overline{\psi} = 0 \tag{41}$$

in which the refractive index n now given by

$$n^2 = \frac{k^2}{k_0^2} \left(1 + A|\nabla_h h|^2 + B\nabla_h^2 h\right) \tag{42}$$

and A and B are known but complicated functions of h (see [14] for example). Comparison of (32), (33) with (41), (42) shows that the structure of the Shallow Water Equation and the MMSE are identical and the equations differ only in the complexity of the coefficients multiplying the higher order terms. In principle, this means that any problem that is considered under the Shallow Water Equations should also be considered under a mild-slope approximation where the range of values of kh is unrestricted.

We shall also introduce another form the the MMSE later on.

3 Transformation media approach

The approach taken by [30] to cloaking has since seen widespread use. As in the case of [19] it is also based on a mapping between a space where waves propagate uninterrupted to a distorted space surrounding an object. It had previously been shown in [41] how Maxwell's equations of electromagnetics were invariant under a coordinate transformation, provided material parameters (permittivity and permeability in this case) could be interpreted as tensors encoding a spatially-varying anisotropic medium. We shall shortly see how the same approach can be applied in the water wave problem and the difficulties it introduces.

Soon after the paper of [41], [30] showed how such material parameters could be achieved using sub-wavelength split ring resonators; this was experimentally demonstrated a year later in [38]. Thus the modern science of metamaterials was born and it has developed rapidly since. We shall discuss such structures in the water wave context shortly – the point is that it is no good devising a cloak if it cannot be realised.

We shall work with the Shallow Water Equations initially but will comment on the MMSE towards the end, having already made the point in §2.4 that what you can do for $kh \ll 1$ should extend to all kh under an equivalent MSE model.

3.1 The Shallow Water Equations revisited

It helps to return to the derivation of the Shallow Water Equations from first principles (see [24, §3.5]). Thus, if the wavelength is long compared to the depth and the bed gradients are small compared to the wavelength it is resonable to assume that the fluid velocity vector is approximately two-dimensional, or $\mathbf{u}(x, y, z, t) \approx (\mathbf{v}(x, y, t), 0)$ where $\mathbf{v} = (u(x, y, t), v(x, y, t))$. That is, there is negligible dependence on the depth and negligible vertical velocity. If the depth is $h(x, y)$ and the surface elevation is $\zeta(x, y, t)$ and $|\zeta| \ll h$ then conservation of mass is expressed as

$$\rho\zeta_t + \nabla_h \cdot (\rho h\mathbf{v}) = 0 \tag{43}$$

where ρ is the fluid density, $\rho h\mathbf{v}$ is the flux and the momentum equation is

$$\rho\mathbf{v}_t = -\nabla_h(\rho g\zeta). \tag{44}$$

and the pressure is approximately hydrostatic. Combining (43) and (44) gives

$$\rho\zeta_{tt} = \nabla_h \cdot (h\nabla_h(\rho g\zeta)) \tag{45}$$

and after assuming time harmonic motion with angular frequency ω with $\rho g\zeta = \Re\{\eta \mathrm{e}^{-\mathrm{i}\omega t}\}$ we return to

$$\nabla_h \cdot (h\nabla_h\eta) + \frac{\omega^2}{g}\eta = 0 \tag{46}$$

as in (30). Now imagine waves travelling in different directions are able to experience different material properties. For example, imagine the fluid depth h to be multi-valued so that waves travelling in the x-direction experience a depth $h_1(x, y)$ whilst waves travelling in the y-direction experience a depth $h_2(x, y)$. The same arguments could apply to either gravity or the density ρ. To illustrate the ideas let us assume that ρ and g are constant and h is allowed to be anisotropic in the manner suggested. Now mass conservation (43) needs to be modified to reflect the fluxes in x and y directions are different. Thus we can write

$$\zeta_t + \nabla_h \cdot (\mathsf{h}\mathbf{v}) = 0 \tag{47}$$

where h is a rank-2 tensor given by

$$\mathsf{h} = \begin{pmatrix} h_1 & 0 \\ 0 & h_2 \end{pmatrix} \tag{48}$$

and following through the derivation as before results in the Shallow Water Equation modified for anisotropic depth:

$$\nabla_h \cdot (\mathsf{h}\nabla_h\eta) + \frac{\omega^2}{g}\eta = 0. \tag{49}$$

We remark that full anisotropy can also be considered in which h has off-diagonal entries. This would require development of a medium in which fluid flow in one direction will induce mass flux in a perpendicular direction. Realisations of fluid metamaterials are considered in §3.4.

3.2 Mapping

We shall work in plane polar coordinates from now on. This means that anisotropy will apply in radial and angular directions rather than in Cartesian directions as considered in 3.1.

We start with waves propagating in the direction $\theta = 0$ over a flat bed $h = h_0$ without scattering obstacles. The governing equation (31), with the shallow water assumption $k_0 = \omega^2/(gh_0)$, written in polars is

$$\frac{1}{r}\frac{\partial}{\partial r}\left(r\frac{\partial \eta}{\partial r}\right) + \frac{1}{r^2}\frac{\partial^2 \eta}{\partial \theta^2} + k_0^2\eta = 0 \tag{50}$$

and the solution is $\eta(r,\theta) = \mathrm{e}^{\mathrm{i}k_0 x} = \mathrm{e}^{\mathrm{i}k_0 r\cos\theta}$.

Now consider a mapping $(r,\theta) \to (\varrho,\theta)$ where $r = f(\varrho)$ for $0 < r < b$ and $r = \varrho$ otherwise, such that $r = b$ is mapped to $\varrho = b$ and $r = 0$ is mapped to $\varrho = a$. Then (50) remains unchanged for $r > b$ and for $0 < r < b$ it is mapped to

$$\frac{1}{f'f}\frac{\partial}{\partial \varrho}\left(h_0\frac{f}{f'}\frac{\partial \widetilde{\eta}}{\partial \varrho}\right) + \frac{1}{f^2}\frac{\partial}{\partial \theta}\left(h_0\frac{\partial \widetilde{\eta}}{\partial \theta}\right) + K\widetilde{\eta} = 0 \tag{51}$$

for $a < \varrho < b$ where $\widetilde{\eta}(\varrho,\theta) = \eta(r,\theta)$.

3.3 A linear map

The map suggested by [30] is defined by

$$f(\varrho) = \frac{b(\varrho - a)}{b - a}. \tag{52}$$

Using this in (51) gives

$$\frac{1}{\varrho}\frac{\partial}{\partial \varrho}\left(\varrho h_1\frac{\partial \widetilde{\eta}}{\partial \varrho}\right) + \frac{1}{\varrho}\frac{\partial}{\partial \theta}\left(h_2\frac{1}{\varrho}\frac{\partial \widetilde{\eta}}{\partial \theta}\right) + \widetilde{K}\widetilde{\eta} = 0 \tag{53}$$

where

$$h_1 = h_0(1 - a/\varrho), \qquad h_2 = h_0/(1 - a/\varrho) \tag{54}$$

and

$$\widetilde{K} = K(1 - a/\varrho)/(1 - a/b)^2. \tag{55}$$

We see that (53) is a Shallow Water Equation in the form given by (49) in polar coordinates where h_1 and h_2 are spatially-varying anisotropic depths experienced by waves moving in radial and angular directions respectively.

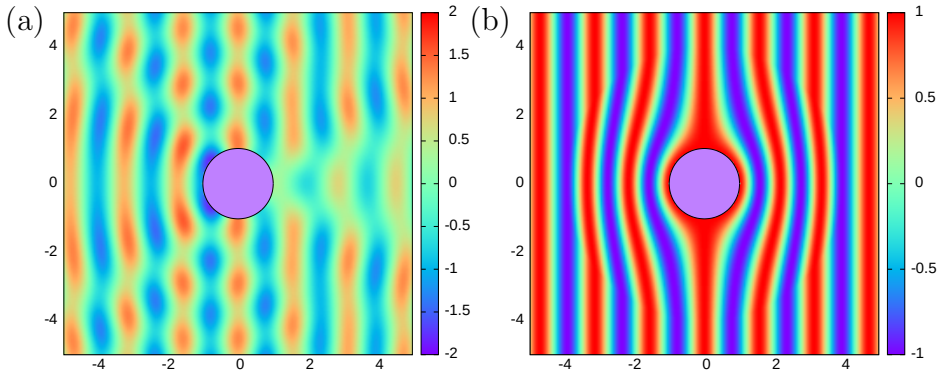

Figure 3: (a) Snapshot of surface wave elevation for scattering by an uncloaked vertical cylinder ($a = 1$, $k_0 = 4$); and (b) perfect cloaking under a linear transformation with depths (54) and gravity implied by (55) with cloak size $b = 4$.

On the edge of the cloak, the conditions in the unmapped system are that η and $h_0\eta_r$ are continuous across $r = b$. Under the general mapping $r = f(\varrho)$ this implies $\widetilde{\eta}$ is continuous and

$$\frac{h_0}{f'}\widetilde{\eta}_\varrho|_{\varrho=b^-} = h_0\widetilde{\eta}_\varrho|_{\varrho=b^+}. \tag{56}$$

For the map (53) this reduces to

$$h_1\widetilde{\eta}_\varrho|_{\varrho=b^-} = h_0\widetilde{\eta}_\varrho|_{\varrho=b^+} \tag{57}$$

which is the exactly the physical shallow water flux condition required of $\widetilde{\eta}$ at the edge of the cloak. On the cylinder, $\varrho = a$, $h_1\widetilde{\eta}_\varrho = 0$ which confirms no flux into the cylinder in the mapped problem. A snapshot in time of the surface elevation for the linear transformation is shown in Fig. 3.

In the context of water waves [11] performed a transformation of the Laplacian ∇_h^2 using homogenisation theory in which the cloaking region $a < \varrho < b$ is filled with a fluid metamaterial consisting of an annular array of narrow vertical posts embedded in the fluid. They were able to show how the distribution of posts could be varied to mimic a diagonal tensor h with a given radial variation. It is not clear if [11] were using their metamaterial annular array of posts to mimic an effective anisotropic depth, or appealing

to a different underlying physical mechanism to vary the phase speed within the cloak. In any case, [11] proposed a different prescription of the diagonal tensor entries to (54) and held their value of $\widetilde{K}$ fixed. Nevertheless, they produced experiments to show that a degree of cloaking could be achieved.

The mapped variables (54) and (55) are identical to those given in [9] who considered cloaking in two-dimensional acoustics. In this case the governing equations are analagous to the Shallow Water Equations with density replacing depth and the bulk modulus replacing gravity. They are also the same as TE-polarized waves in electromagnetics specified by [30] with permeability and permittivity taking the place of depth and the reciprocal of gravity.

3.4 Metamaterial depth and gravity

Under the linear mapping of the previous section (55) shows that a cloak requires an effective gravity given by

$$\widetilde{g} = g(1 - a/b)^2/(1 - a/\varrho). \tag{58}$$

Such an effect can be realised in water waves since gravity enters the equations of motion through one of the two conditions on the free surface. Thus, one can load the free surface to mimic the effect of changing gravity. This has been done in early papers modelling the effect of floating broken ice on the ocean surface. For example, [17] show that if the surface is loaded with a floating mass m, the term in ω^2/g occupied by gravity is replaced by

$$g(1 - m\omega^2/\rho g). \tag{59}$$

By allowing $m(\varrho) \geq 0$ to vary, (59) implies a reduction in the effective gravity. Unfortunately the specification in (58) requires gravity to vary above and below the reference value of g as $a < \varrho < b$.

It is also worth mentioning the work of [15] who demonstrated that doubly periodic sub-wavelength arrays of split ring resonators acting as Helmholtz resonators could be used to change the effective gravity felt by waves.

With regard to realising an anisotropic metamaterial depth, we have already referred to the method used by [11] in which homogenisation theory applied a sub-wavelength array of vertical posts can mimic the effects of anisotropic depth variations. The same methodology was applied by [10] in creating an invisiblity carpet for water waves in a channel: a device for hiding an obstacle placed in front of a plane wall from the far-field observer.

An alternative sub-wavelength realisation of a metamaterial water depth, again developed using homogenisation theory, was presented by [4]. They considered how to redirect a propagating water wave through an angled junction in a parallel-walled waveguide without reflection. Crucially their transformation was volume-preserving with the implication that gravity is unaffected by the mapping. The physical realisation of their metamaterial depth was comprised of a microstructured corrugated rectangular bed profile. A similar technique was used by [8] who demonstrated how a metamaterial depth could be used to rotate an incident wave field.

A further possible realisation of the anisotropic depth, such as the one demanded by (54), can be performed using two interlocking arrays of thin closely-spaced vertical fins. One set of fins are arranged radially so that their height follows the prescription given by the function h_2 and the second set are arranged in a circular pattern with heights following the function h_1. Then waves travelling radially are not influenced by the radial fins but experience the depth profile of the circular fins and vice versa.

3.5 A nonlinear map

More recently, [42] suggested an alternative mapping function for the cloak in order to cope with the difficulty of having to alter gravity this arising from the linear map. Instead of (52) they used

$$f(\varrho) = b\sqrt{\frac{\varrho^2 - a^2}{b^2 - a^2}} \tag{60}$$

in (51) and this results in (53) with

$$h_1 = h_0(1 - a^2/b^2)(1 - a^2/\varrho^2), \qquad h_2 = h_0(1 - a^2/b^2)/(1 - a^2/\varrho^2) \tag{61}$$

and now $\widetilde{K} = K$. That is, there appears to be no requirement that gravity is altered under this nonlinear mapping.

However, on the boundary of the cloak the flux matching condition (56) gives

$$\frac{h_0}{1 - a^2/b^2}\widetilde{\eta}_\varrho|_{\varrho=b^-} = h_0\widetilde{\eta}_\varrho|_{\varrho=b^+} \tag{62}$$

and the prefactor on the left-hand side is *not* $h_1(b)$ as is required for a physical flux condition, i.e. there is a mismatch in the flux at the boundary of the cloak of $(1 - a^2/b^2)$.

One way to overcome this difficulty is to rescale h_1 and h_2 in (61) by a factor of $(1-a^2/b^2)$. In doing so, one must also rescale K and so we return to (53) with a transformed value of

$$\widetilde{K} = K/(1-a^2/b^2). \tag{63}$$

This implies gravity should be rescaled in the cloak by a constant factor of $(1-a^2/b^2)$. This reduction in effective gravity can be implemented using the mass loading solution proposed in §3.4.

In [42] they argue instead that the flux mismatch factor of $(1-a^2/b^2)$ is small when $b \gg a$ and computations show that cloaking improves significantly as the b/a, the size of the cloaking increases. This will be confirmed by the calculations below.

As [42] show, the effect of the flux mismatch on scattering of waves can be analysed directly by solving the problem analytically. A plane incident wave from infinity is scattered by a cloak defined by the functions in (61) when the physical flux condition (57) is enforced. Solutions outside the cloak where the depth is h_0 are written

$$\widetilde{\eta}(\varrho,\theta) = \sum_{n=-\infty}^{\infty} (\mathrm{i}^n J_n(k_0\varrho) + a_n H_n^{(1)}(k_0\varrho))\mathrm{e}^{\mathrm{i}n\theta}, \qquad \varrho > b \tag{64}$$

as in §1.3 for the problem of scattering by a cylinder and a_n are scattering coefficients to be determined. If the cloak were perfect, all a_n would be zero.

In $a < \varrho < b$ the most general solution to (53), which is bounded on the cylinder $\varrho = a$ can be written

$$\widetilde{\eta}(\varrho,\theta) = \sum_{n=-\infty}^{\infty} b_n J_n\left(k_0 b\sqrt{\frac{\varrho^2-a^2}{b^2-a^2}}\right)\mathrm{e}^{\mathrm{i}n\theta}. \tag{65}$$

The flux into the cylinder is $\lim_{\varrho\to a}(h_1\widetilde{\eta}_\varrho) = 0$ as required. It is also interesting to note that $\widetilde{\eta}(a,\theta)$, the complex wave amplitude around the cylinder, is constant.

Matching $\widetilde{\eta}(b,\theta)$ for $-\pi < \theta < \pi$ from (64) and (65) gives

$$\mathrm{i}^n J_n(k_0 b) + a_n H_n^{(1)}(k_0 b) = b_n J_n(k_0 b). \tag{66}$$

Then we apply (57) to (64) and (65) to get

$$\mathrm{i}^n J_n'(k_0 b) + a_n H_n^{(1)'}(k_0 b) = b_n(1-a^2/b^2) J_n'(k_0 b). \tag{67}$$

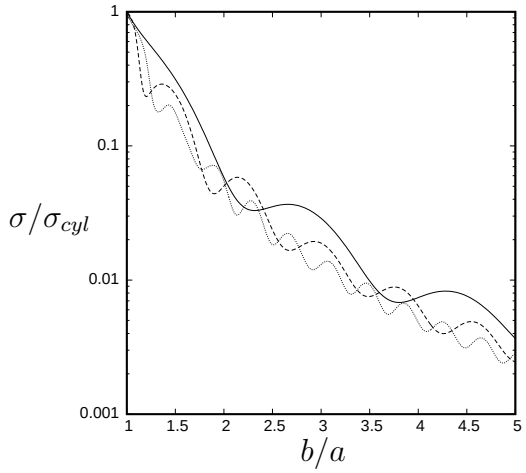

Figure 4: Normalised cloaking factor σ/σ_{cyl} for the nonlinear mapping against cloak size b/a with $k_0 a = 1$ (solid), 2 (dashed) and 4 (dotted).

Eliminating b_n gives

$$a_n = \frac{\mathrm{i}^n (a^2/b^2) J_n'(k_0 b) J_n(k_0 b)}{-2\mathrm{i}/(\pi k_0 b) - (a^2/b^2) J_n'(k_0 b) H_n^{(1)}(k_0 b)} \tag{68}$$

after using a Wronskian relation for Bessel functions. If the flux mismatch were not present the factor $(1 - a^2/b^2)$, on the right-hand side of (67) would be replaced by 1 and this would result in $a_n = 0$ for all n whilst $b_n = \mathrm{i}^n$ – equivalent to a perfect cloak.

We remark that the cloaking solution above is not restricted to plane waves. For example, the problem of a wave source placed at $r = c$, $\theta = 0$ outside the cloak can be considered by replacing the Jacobi-Anger representation of a plane wave train in (15) by

$$\sum_{n=-\infty}^{\infty} H_n^{(1)}(k_0 r_>) J_n(k_0 r_<) \mathrm{e}^{\mathrm{i}n\theta} \tag{69}$$

using Graf's addition theorem where $r_< = \min\{r, c\}$, $r_> = \max\{r, c\}$. The result is that the factor i^n carried throughout the previous calculation is replaced by $H_n^{(1)}(k_0 c)$.

From (64), (22) the scattering cross-section is

$$\sigma = \frac{1}{2\pi} \sum_{n=-\infty}^{\infty} |a_n|^2 \tag{70}$$

and hence $\sigma = O((b/a)^{-4})$. Calculations confirm this decay rate and Fig. 4 shows the variation of σ normalised against the scattering cross section of an uncloaked cylinder, σ_{cyl}, given by (23) for different incident wavelengths. Snapshots of the surface elevation for two cloaks of sizes $b = 2a$ and $b = 4a$ with are shown in Fig. 5.

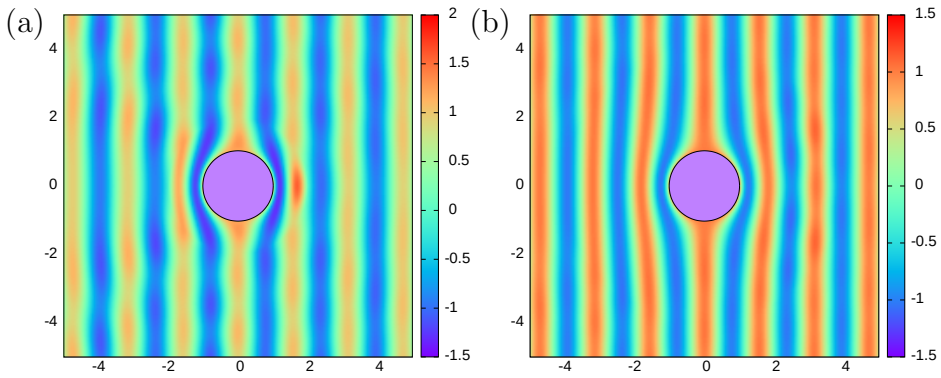

Figure 5: Near-perfect cloaking under a nonlinear transformation with depths given by (61) and gravity unchanged, $a = 1$, $k_0 = 4$ and cloak sizes of (a) $b = 2$ and (b) $b = 4$.

3.6 A note on the Mild-Slope Equations

In §3 we introduced the Modified Mild-Slope Equation (MMSE), given in its original form by (40) and in its canonical form by (41), (42). However, a different mapping of the variable $\psi(x, y)$, proportional to the free surface, was introduced by [32] using $\psi = s(h)\chi$ where $s(h)$ is defined in [32, §2] and results in the transformed MMSE

$$\nabla_h \cdot (k^{-2}\nabla_h \chi) + (1 - \nu(h)|\nabla_h h|^2)\chi = 0 \tag{71}$$

where $v(h)$ is a relatively complicated, but explicit, function of the local depth. There are some advantages of this form of the MMSE. First, terms in

the second derivative of h are eliminated and this means that jump conditions – required in the earlier versions of the MMSE – across discontinuities in the bed slope are redundant. Secondly, [32] calculates that $v(h) < 0.030$ for all $h > 0$ and so the final term in (71) is small. Moreover, as $v(h) \sim O((kh)^2)$ as $kh \to 0$ and it is easy to see that (71) tends to the Shallow Water Equations in this limit. When kh is large $v(h) \sim \mathrm{e}^{-kh}$ and, since $k \sim K$, (71) tends to a wave equation with no depth effects, as expected. As a result solutions of

$$\nabla_h \cdot (k^{-2}\nabla_h \chi) + \chi = 0 \tag{72}$$

are expected to be good approximations to solutions of (71). The advantage of using (72) is that its structure is aligned with the Shallow Water Equation (49), with k determined locally as a function of h via (14).

In particular the transformation media methods outlined in §3.2 can be applied to the MMSE in the form (72) and solutions will be valid not just in the limit of $kh \ll 1$ but for all kh.

For example, following [42] we could apply the transformation media method with the mapping (60) to the define a cloak with radial and angular wavenumbers

$$k_1 = \frac{k_0}{\sqrt{(1 - a^2/b^2)(1 - a^2/\varrho^2)}}, \qquad k_2 = k_0 \sqrt{\frac{1 - a^2/\varrho^2}{1 - a^2/b^2}}. \tag{73}$$

The depths h_1 and h_2 would then be defined by inverting the dispersion relation: $h_i = \tanh^{-1}(K/k_i)/k_i$, $i = 1, 2$. It is anticipated that such a solution would apply beyond the limitations of shallow water theory although it would still suffer the flux mismatch problem discussed in §3.5 and would still be subject to the small-gradient constraint underpinning the mild-slope approximation.

3.7 Other cloaking devices

As demonstrated in the derivation of (46) the fluid density, whether or not it is anisotropic, is not a material parameter in the Shallow Water Equations (nor the full linear theory of §1). Thus spatial variations of density in the horizontal coordinates will not influence wave motion. [16] suggest otherwise, although their governing equations do not appear to relate directly to the Shallow Water Equations. Vertical density stratification fundamentally

alters the governing equations where it is normal to adopt the Boussinesq approximation – see [31], for example.

As previously suggested, instead of (or in addition to) varying the bathymetry, the free surface condition can be altered to control waves and a simple mass-loading model was proposed in §3.4. Another possibility is to place a thin flexible plate on the surface of the water to act as a cloak. The floating thin flexible plate model is widely used by researchers interested in the interaction between ice sheets and ocean waves; for a comprehensive review of work in this area, see [39]. Problems involving waves in thin flexible plates surrounding vertical cylinders have previously been considered in the work of [6] and [20] Also see [2] for scattering problems involving flexible circular plates of varying thickness.

It is common to use Kirchhoff thin plate theory to model a flexible sheet. Even in the simpler problem of a flexible plate *in vacuo*, the fourth-order governing equations are not invariant under a coordinate transformation. The addition of a shallow water layer below the floating elastic plate complicates the underlying equations which increase in derivative order from four to six. For an elastic plate with variable thickness $D(x, y)$ over a variable bed $z = -h(x, y)$, [33] derive mild-slope equations for the reduced two-dimensional potential $\psi(x, y)$ in the fluid. Under the additional simplifying assumption of shallow water the governing equation for ψ is ([33, eqn. (4.9)])

$$(1 - \alpha + \mathcal{L})(\nabla_h \cdot ((h - d)\nabla_h \psi) + K\psi = 0 \tag{74}$$

where $\alpha = K(\rho_s/\rho)D(x, y)$ and ρ_s is the plate density and thickness and $z = -d(x, y)$ represents the underside of the floating plate. In the above

$$\mathcal{L}\psi = \nabla_h^2(\beta\nabla_h^2\psi) - (1 - \nu)(\beta_{xx}\psi_{xx} + \beta_{yy}\psi_{yy} - 2\beta_{xy}\psi_{xy}) \tag{75}$$

where $\beta = ED^3(x, y)/(12\rho g(1-\nu^2))$ represents the bending stiffness in terms of Young's modulus, E, and Poisson's ratio, ν. Of course, one could keep D fixed and vary Young's modulus or Poisson's ratio or vary all three. We note that if the floating plate is removed so that $\alpha = 0$, $d = 0$ and $\mathcal{L} = 0$ in (74) then we simply return to the usual free surface Shallow Water Equation (46).

[43] have suggested an alternative model for the floating plate equation which can be media transformed, following the earlier work of [12] on *in vacuo* thin flexible plates.

We remark that (74) and (75) are derived under the usual assumptions of isotropic elasticity. A derivation that incorporates anisotropic material properties should be performed to assess the feasibility of using a floating flexible plate as a cloak. This is currently the subject of an investigation by Zareei & Alam (personal communication).

4 Full linear theory

Thus far we have only considered approximations to full linear theory in which the complication of the depth dependence and lateral boundary conditions have been removed. Cloaking is the science of rendering objects invisible and there is no guarantee that a cloak developed under a reduced model will be effective in an unapproximated environment. One must be especially cautious when the limits on the assumptions forming the basis of an underlying model have been exceeded.

4.1 Conformal mapping

In this section the implementation of a mapping from (x, y, z) to (u, v, w) space in the full linearised water wave boundary-value problem is described. As in §2.3 a conformal mapping in the horizontal plane is introduced by writing $\beta = f(\xi)$ where $\beta = u + \mathrm{i}v$ and $\xi = x + \mathrm{i}y$. Laplace's equation in three-dimensions is preserved by a simultaneous rescaling of the vertical coordinate using $w = |f'|z$. That is $\nabla^2\phi$ is mapped into $\widetilde{\nabla}^2\widetilde{\phi} = 0$ where $\phi(x, y, z) \equiv \widetilde{\phi}(u, v, w)$ and $\widetilde{\nabla}^2 \equiv \partial_{uu} + \partial_{vv} + \partial_{ww}$. The mapped free surface boundary condition (9) is

$$\widetilde{\phi}_w - \widetilde{K}\widetilde{\phi} = 0, \qquad \text{on } w = 0 \tag{76}$$

where $\widetilde{K} = K/|f'|$. The bed $z = -h(x, y)$ is mapped to the boundary $w = -\widetilde{h}(u, v) \equiv |f'|h$ and the transformation of the general bed condition (11) results in

$$\widetilde{\phi}_w + \{\widetilde{\nabla}_h\widetilde{h} + |f'|\widetilde{h}\widetilde{\nabla}_h(|f'|^{-1})\} \cdot \widetilde{\nabla}_h\widetilde{\phi} = 0, \qquad \text{on } w = -\widetilde{h}. \tag{77}$$

In (x, y, z) space defined by a flat bed of depth h_0 in the presence of a thin impermeable vertical barrier $-2a < x < 2a$, $y = 0$, $-h_0 < z < 0$, plane waves propagating in the direction $\theta = 0$ are described by the potential ϕ_{inc}

in (15). The mapping of the barrier to a cylinder in (u, v, w) space is given by

$$\xi = \beta + \frac{a^2}{\beta} \tag{78}$$

or $\beta = f(\xi) = \frac{1}{2}(\xi + \sqrt{\xi^2 - 4a^2})$. Then $f'(\xi) = \beta^2/(\beta^2 - a^2)$ and

$$|f'| = \frac{1}{\sqrt{1 + a^4/\varrho^4 - 2a^2 \cos 2\varphi/\varrho^2}} \tag{79}$$

when $\beta = \varrho e^{i\varphi}$. Apart from the singular points at $\beta = \pm a$, $\widetilde{h} = h_0|f'|$ defines a physically-realisable variable depth. Here $\widetilde{K} = K/|f'|$ represents a variation of effective gravity on the free surface which both falls and rises above the far-field value, g. Thus the mass-loading model described in §3.4 cannot be used to realise the surface condition (76).

When $h = h_0$ is a constant, the transformed bed condition (77) simplifies to

$$\widetilde{\phi}_w = 0, \qquad \text{on } w = -\widetilde{h}(u, v) = -h_0|f'|. \tag{80}$$

This is *not* the usual condition (c.f. (11)) $\widetilde{\phi}_w + \widetilde{\nabla}_h \widetilde{h} \cdot \widetilde{\nabla}_h \widetilde{\phi} = 0$ required on a natural bed. Thus, in addition to the variable surface condition, one would also need to design a metamaterial bed to realise (80) in order to cloak a cylinder under full linear theory using the mapping proposed here. For example, such a bed could be formed by a vertical cascade of narrowly-spaced thin horizontal plates immersed within the fluid whose edges are designed to follow the profile $\widetilde{h} = h_0|f'|$ where f' is given by (79). Surface waves would feel the macroscopic effect of the variable bathymetry but locally the fluid would satisfy a vertically-directed no-flow condition.

The solution described above was initially formulated in [34] although the details and the description of the metamaterial bed in the paragraph above are new.

4.2 A direct approach

In this section the approach reported in [35] used to cloak a circular cylinder without relying on metamaterials is presented. Instead of designing a cloak which bends waves around the cylinder it relies on combining wave diffraction effects from the cylinder and an annular region of variable bathymetry to destroy outgoing waves in all directions. This approach shares similarities

with the one used by [1] in an electromagnetic context in which they coated a dielectric cylinder with an annular dielectric with constant properties and showed how the scattering cross-section could be reduced significantly.

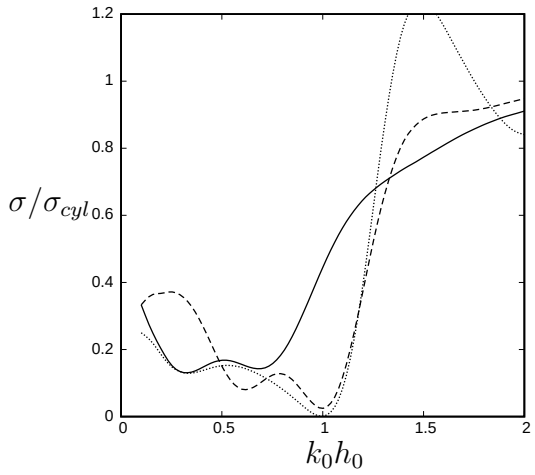

Figure 6: Cloaking factor against wavenumber under full linear theory calculations for axisymmetric beds ($Q = 1$) optimised for cloaking at $k_0h_0 = 1$, $a/h_0 = \frac{1}{2}$ $b/h_0 = 5$ with $P = 2$ (solid), $P = 4$ (dashed) and $P = 8$ (dotted).

The work published in [14], developed to investigate the focusing of water waves over a bathymetric lens using the MMSE, was adapted by [34] to include a vertical cylinder. The shape of the bed in the annular cloak $a < r < b$ was expanded in a weighted set of prescribed modal functions:

$$h(r,\theta) = \sum_{p=1}^{P}\sum_{q=1}^{Q} \alpha_{pq} f_p(r) \cos 2(q-1)\theta \tag{81}$$

in which

$$f_p(r) = T_{2p}\left(\frac{b-r}{b-a}\right) - (-1)^p \tag{82}$$

where T_p are Chebychev polynomials. This choice implies that $h_r = 0$ at $r = b$ so that there is no discontinuity in bed slope at the edge of the cloak, a feature which was chosen for convenience as it avoided the need to implement jump conditions in the MMSE solution. Chebychev polynomials were chosen because it was anticipated that greater resolution of the bed may be required

close to the cylinder boundary $r = a$. The incident wave was assumed to be aligned with $\theta = 0$ and only even angular modes were used in the expansion (81) by appealing to ideas of time-reversal symmetry.

In (81) the $P \times Q$ coefficients α_{pq} were treated as free parameters in a numerical multi-parameter optimisation whose objective function to be minimised was the normalised "cloaking factor" C defined to be the scattering cross-section σ of the cloaked bed divided by σ_{cyl}, say, for uncloaked bed, given by (23).

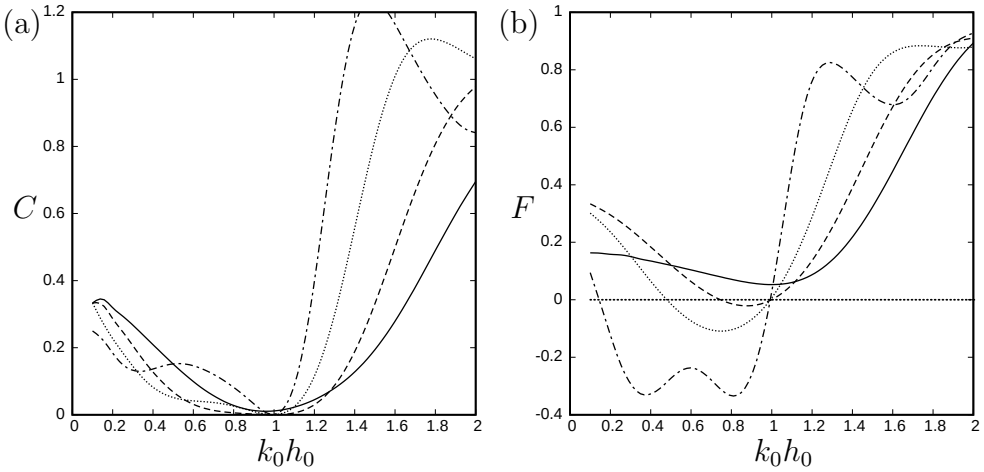

Figure 7: In (a) the cloaking factor $C = \sigma/\sigma_{cyl}$ and in (b) the normalised mean drift force on the cylinder, F, both plotted against against wavenumber for an axisymmetric bed, $Q = 1$, $P = 8$ optimised to cloak at $k_0h_0 = 1$ with $a/h_0 = \frac{1}{2}$ and $b/h_0 = 2$ (solid), 3 (dashed), 4 (dotted), 5 (chained).

In the studies of [35] results were presented for cloaking targeted at a particular frequency and geometry ($k_0h_0 = 1$, $a/h_0 = \frac{1}{2}$) although other parameters were considered in numerical experiments leading to that publication.

The initial work using the MMSE was presented in [34] suggested that cloaking factors could be progressively reduced towards zero as the number of degrees of freedom defining the bed were increased. A year later, [26] published work adopting the same principles and methodology of [34] but using a modified version of the fully three-dimensional boundary element code, WAMIT. The work was combined in the paper of [35] where numerical results supported the hypothesis that the cloaking factor could be reduced to

zero as the number of degrees of freedom in the bed were increased under full linear theory – see Fig. 6 for example. That work also alluded to the fact that cloaking was sensitive to small changes in the bathymetry and the comparison between MMSE and full linear theory was shown to be generally quite poor due to the large gradients predicted in cloaking beds. This comment serves to act as a cautionary note regarding the predictions made in §3 under depth-reduced models.

Fig. 7(a) shows the effect of the size of the cloak on the cloaking factor for cloaking-optimised axisymmetric beds. [35] demonstrated that cloaking is best for $b \approx 5a$ whilst the cloaking effect can also seen to be broadbanded. Fig. 7(b) illustrates the significant reduction in the mean second-order drift force on the cylinder (normalised against an uncloaked cylinder), especially around the cloaking wavenumber $k_0 h_0 = 1$.

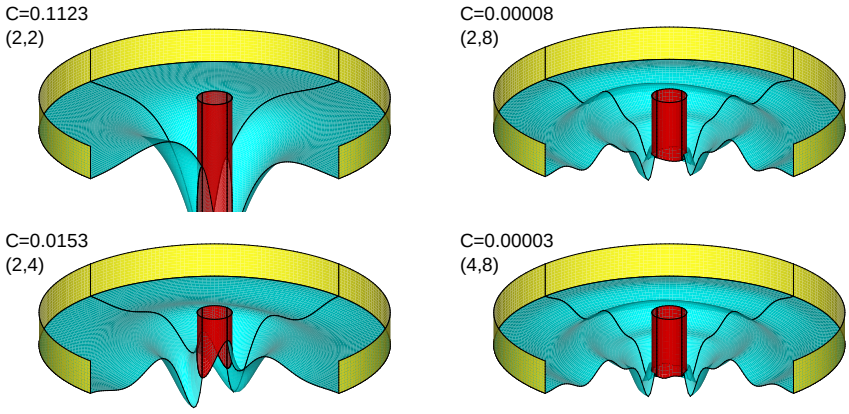

Figure 8: Beds optimised to cloak at $k_0 h_0 = 1$ for different values of (Q, P) with $a/h_0 = \frac{1}{2}$, $b/h_0 = 5$. Values of cloaking factor $C = \sigma/\sigma_{cyl}$ achieved in each case are shown. The yellow boundary depicts the edge of cloak.

[35] also showed that convergence towards perfect cloaking was improved by breaking axisymmetry and letting $Q > 1$. See Figs. 8.

4.3 Extensions to the direct approach

[27] later developed a double-precision version of the original single-precision code WAMIT to numerically investigate alternative ways of cloaking a cylin-

der under full linear theory. This included, amongst many other examples, surrounding the vertical cylinder to be cloaked with a concentric circular ring of N fixed truncated surface-piercing circular cylinders. Again, a numerical optimisation procedure was used to tune a number of free parameters used to encode the geometric configuration of the cloak. [27] was able to show that whilist an axisymmetric ring quickly reduced the cloaking factor as N increased, significant improvements to cloaking factors could be achieved by breaking the axisymmetry of the cloak, with values of $C = 1.1 \times 10^{-9}$ being reported.

The numerical evidence seemed to suggest that perfect cloaking is possible. However, [23] provides a formal proof that, under certain conditions, perfect cloaking is not possible. The proof applies to a specific class of cloaks comprised of elements individually satisfying the so-called "John condition" (e.g. see [18]), Geometrically, the John condition is satisfied if lines projected vertically downwards from all points on the free surface meet the flat bed without intersecting a body in the fluid. This is a powerful result. Unfortunately, [27]'s configuration of N surface-piercing truncated cylinders discussed in the previous paragraph does satisfy the John condition and so it transpires that perfect cloaking is not possible in this example despite the extremely low cloaking factors calculated. This also puts in doubt the suggestion that perfect cloaking is achievable in the earlier example of [35] involving variable bathymetry.

5 Summary

In this article, I have tried to present a range of different approaches that can be used to investigate the cloaking in water waves. This includes the simplified models of ray theory, shallow water theory and the mild-slope approximation in addition to the consideration of full linear wave theory. It has been shown how mapping methods may be applied within the framework of each of these models. It has also been shown how metamaterials can be designed in water wave problem to realise unnatural boundary conditions that emerge from these mappings such as anisotropic water depth and variable effective gravity.

The most successful attempts at creating a cloak for a circular cylinder seem to be: (i) using the nonlinear transformation of [42] shown in §3.5 within the framework of the shallow water approximation and (ii) numerical

optimisation of bathymetry or other structures embedded in the fluid that form a cloak under full linear theory. The latter has the advantage of being exact and realisable without metamaterial parameters. The former has the advantage that they bend waves around the cylinder rather than relying on the cylinder for multiple interference effects that are integral to the cloak.

The transformation media approach and, more generally, the adoption of metamaterials in water waves can provide an interesting range of new possibilities to water wave problems. For example, one might consider mapping the well-known explicit Stokes edge wave solution (or its shallow water approximation) along a plane sloping beach under a coordinate transformation into circular coordinates to provide a solution in which waves are trapped to a circular island by a "metamaterial beach".

References

[1] Alù, A. and Engheta, N. (2005). Achieving transparency with plasmonic and metamaterial coatings. *Phys. Rev. E.* **72**, 016623.

[2] Bennetts, L. G., Biggs, N. R. T. and Porter, D. (2009). Wave scattering by an axisymmetric ice floe of varying thickness. *IMA. J. Appl. Math.* **74**, pp. 273–295.

[3] Berkhoff, J. C. W. (1973). Computation of combined refraction-diffraction. *Proc. 13th Conf. on Coastal Engng., July 1972, Vancouver, Canada*, vol. 2, pp. 471–490. ASCE.

[4] Berraquero, C. P., Maurel, A., Petitjeans, P. and Pagneux, V. (2013). Experimental realization of a water-wave metamaterial shifter. *Phys. Rev. E.* **88**, 051002.

[5] Bobinksi, T. M. (2016). *Metamateriaux pour les ondes a la surface de l'eau (Metamaterials for water waves)* (Ph.D. Thesis, Universite Pierre et Marie Curie.)

[6] Brockenhurst, P., Korobkin, A. A. and Parau, E. I. (2011). Hydroelastic wave diffraction by a vertical cylinder. *Phil. Trans. Roy. Soc. Lond. A.* **369**, pp. 2832–2851.

[7] Chamberlain, P. G. and Porter, D. (1995). The modified mild-slope equation. *J. Fluid Mech.* **291**, pp. 393–407.

[8] Chen, H., Yang, J., Zi, J. and Chan, C. T. (2009). Transformation media for linear liquid surface waves. *EuroPhys. Lett.* **85**, 24004.

[9] Cummer, S. A. and Schurig, D. (2007). One path to acoustic cloaking. *New J. Phys.* **9**(45), pp. 1–8.

[10] Dupont, G., Kimmoun, O., Molin, B. Guenneau, S. and Enoch, S. (2015). Numerical and experimental study of an invisibility carpet in a water channel. *Phys. Rev. E.* **91**, 023010.

[11] Farhat, M., Enoch, S., Guenneau, S. and Movchan, A. (2008). Broadband cylindrical acoustic cloak for linear surface waves in a fluid. *Phys. Rev. Lett.* **101**, 134501.

[12] Farhat, M., Guenneau, S. and Enoch, S. (2009). Ultrabroadband elastic cloak in thin plates. *Phys. Rev. Lett.* **103**, 024301.

[13] Farhat, M., Guenneau, S., Enoch, S. and Movchan, A. (2010). All-angle-negative-refraction and ultra-refraction for liquid surface waves in 2D phononic crystals. *J. Comp. Appl. Math.* **234**(6), pp. 2011–2019.

[14] Griffiths, L. S. and Porter, R. (2012). Focusing of surface waves by variable bathymetry. *Appl. Ocean Res.* **34**, pp. 150–163.

[15] Hu, X., Chan, C. T., Ho, K.-M. and Zi, J. (2011). Negative effective gravity in water waves by periodic resonator arrays. *Phys. Rev. Lett.* **106**, 174501.

[16] Iida, T. and Kashiwagi, M. (2016). Shallow Water Cloaking with Anisotropic Fluid. *Proc. 31st Int. Workshop on Water Waves and Floating Bodies, Michigan, USA.* pp. 65–68.

[17] Keller, J. B. and Goldstein, D. (1953). Water wave reflection due to surface tension and floating ice. *Trans. American Geophys. Union.* **34**(1), pp. 43–48.

[18] Kuznetsov, N., Maz'ya, V. and Vainberg, B. (2002). *Linear Water Waves.* Cambridge University Press.

[19] Leonhardt, U. (2006). Optical conformal mapping. *Science* **312**, 1777.

[20] Malenica, S. and Korobkin, A. A. (2003). Water wave diffraction by vertical circular cylinder in partially frozen sea. *Proc. 18th Int. Workshop on Water Waves and Floating Bodies, Le Croisic, France.*

[21] Maruo, H., (1960). The drift of a body floating on waves. *J. Ship Res.* **4**, 1–10.

[22] McCamy, R. C. and Fuchs, R. A. (1954). Wave forces on a pile: A diffraction theory. *Tech. Memo.* **69**, U.S. Army Board, U.S. Army Corp. of Eng.

[23] McIver, M. (2014). The scattering properties of a system of structures in water waves. *Quart. J. Mech. Appl. Math.* **67**(4), pp. 631–639.

[24] Mei, C. C., Stiassnie, M. and Yue, D. K.-P. (2005). *Theory and Applications of Ocean Surface Waves. Part 1: Linear Aspects.* (World Scientific Publishing Co. Pte. Ltd.)

[25] Miles, J. W. and Gilbert, F. (1968). Scattering of gravity waves by a circular dock. *J. Fluid Mech.* **34**, pp. 783–793.

[26] Newman, J. N. (2012). Scattering by a cylinder with variable bathymetry. *Proc. 27th Int. Workshop on Water Waves and Floating Bodies, Copenhagen, Denmark.*

[27] Newman, J. N. (2014). Cloaking a circular cylinder in water waves. *Euro. J. Mech B/Fluids* **47**, pp. 145–150.

[28] Pendry, J. B. (2000). Negative refraction makes a perfect lens. *Phys. Rev. Lett.* **85**(18), pp. 3966–3969.

[29] Pendry, J. B., Holden, A. J., Robbins, D. J. and Stewart, W. J. (1999). Magnetism from conductors and enhanced nonlinear phenomena. *IEEE. Trans. Microwave Theory and Techniques* **47**(11), pp. 2075–2084.

[30] Pendry, J. B., Schurig, D. and Smith, D. R. (2006). Controlling Electromagnetic Fields. *Science* **312**, 1780.

[31] Phillips, O. M. (1977). *The Dynamics of the Upper Ocean (2nd Edition).* Cambridge University Press.

[32] Porter, D. (2003). The mild-slope equations. *J. Fluid Mech.* **494**, pp. 51–63.

[33] Porter, D. and Porter, R. (2005). Approximations to wave scattering by an ice sheet of variable thickness over undulating bed topography. *J. Fluid Mech.* **509**, pp. 145–179.

[34] Porter, R. (2011). Cloaking of a cylinder in waves. *Proc. 26th Int. Workshop on Water Waves and Floating Bodies, Athens, Greece.* pp. 169–173.

[35] Porter, R. and Newman, J. N. (2014). Cloaking of a vertical cylinder in waves using variable bathymetry. *J. Fluid Mech.* **750**, pp. 124–143.

[36] Shelby, R. A., Smith, D. R. and Schultz, S. (2001). Experimental verification of a negative index of refraction. *Phys. Rev. Lett.* **292**(6), pp. 77–79.

[37] Smith, R. and Sprinks, T. (1975). Scattering of surface waves by a conical island. *J. Fluid Mech.* **72**, pp. 373–384.

[38] Smith, D. R., Padilla, W. J., Vier, D. C., Nemat-Nasser, S. C. and Schultz, S. (2000). Composite medium with simultaneously negative permeability and permittivity. *Phys. Rev. Lett.* **84**(18), 4184.

[39] Squire, V. A. (2007). Of ocean waves and sea-ice revisited. *Cold Regions Sci. Tech.* **49**(2), pp. 110–133.

[40] Wang, Z., Zhang, P., Nie, X. and Zhang, Y. (2015). Manipulating water wave propagation via gradient index media. *Sci. Rep.* **5**, 16846.

[41] Ward, A. J. and Pendry, J. B. (1996). Refraction and geometry in Maxwell's equations *J. Mod. Opt.* **43**(4), pp. 773–793.

[42] Zareei, A. and Alam, M.-R. (2015). Cloaking in shallow-water waves via nonlinear medium transformation. *J. Fluid Mech.* **778**, pp. 273–287.

[43] Zareei, A. and Alam, R. (2016). Cloaking by a floating thin plate. *Proc. 31st Int. Workshop on Water Waves and Floating Bodies, Michigan, USA.* pp. 197–200.